JOURNAL OF GUIDANCE, CONTROL, AND DYNAMICS
Vol. 18, No. 2, March–April 1995

Linear-Quadratic-Gaussian-Based Controller Design for Hubble Space Telescope

Emmanuel G. Collins Jr.*
Florida A&M University/Florida State University, Tallahassee, Florida 32316
and
Stephen Richter†
Harris Corporation, Melbourne, Florida 32902

Large changes in the thermal environment as the Hubble Space Telescope (HST) orbits Earth cause thermal distortion in the solar arrays that in turn cause the solar arrays to vibrate. The original HST controller was not designed to attenuate disturbances due to vibration of flexible members of the HST, and hence the solar array motions led to very noticeable degradation in pointing control. Using classical techniques, Marshall Space Flight Center in conjunction with Lockheed Missiles and Space Company developed modified HST controllers that were able to suppress the influence of the vibrations of the solar arrays on the line-of-sight (LOS) performance. Substantial LOS improvement was observed when two of these controllers were implemented on orbit. This paper describes the development of modified HST controllers by using linear quadratic Gaussian (LQG) design. Two design approaches are considered. The first approach is a one-step process that designs a controller that satisfies both the tracking/integral requirements and the disturbance rejection requirements. The second approach, first designs a controller that satisfies the tracking/integral objectives and then designs a parallel controller that preserves the tracking properties while achieving the disturbance rejection properties. The latter approach was used because it was found to more easily lead to high-performance controllers. The results clearly demonstrate that LQG-based controller design is capable of yielding high-performance controllers for the HST.

I. Introduction

THE anticipation of stringent mission performance requirements of future space missions motivated researchers in automatic control to develop control design techniques applicable to flexible space structures since it was anticipated that the controller would have to interact with the flexible modes in order to satisfy the performance objectives. However, all current space missions were designed so that mission success is not dependent on flexible structure control. The Hubble Space Telescope (HST), shown in Fig. 1, was designed so that active structural control was unnecessary. However, flight experience has revealed the need for the controller to interact with the flexible modes.[1] The need arose due to unanticipated vibration of the solar arrays that occurs as a result of distortions in the solar arrays caused by large changes in the thermal environment as the HST orbits Earth.

The original HST controller, essentially a conventional proportional-integral-derivative (PID) controller, was not designed to attenuate disturbances due to vibration of flexible members of the HST. Hence, the solar array vibrations led to very noticeable degradation in the pointing performance. Using classical techniques, Marshall Space Flight Center (MSFC) in conjunction with Lockheed Missiles and Space Company developed modified HST controllers that were able to suppress the influence of the solar array vibrations on the line-of-sight (LOS) performance.[1] Substantial LOS improvement was observed when two of these controllers were implemented on orbit.

Here, we consider the development of modified HST controllers by using linear quadratic Gaussian (LQG) design.[2,3] In what follows, we discuss some of the main options and issues in applying LQG design to the HST design problem. A reduced-order LQG controller is described and, by using a simulation based upon on-orbit data, the control system is seen to have performance comparable to that of a previously developed modified HST controller.

Received Oct. 25, 1993; revision received Feb. 4, 1994; accepted for publication Sept. 6, 1994.

*Associate Professor, Department of Mechanical Engineering.
†Associate Principal Engineer, Government Aerospace Systems Division.

The LQG controller described here was developed using a decentralized "one-loop-at-a-time" approach, as were the modified HST controllers of Ref. 1. However, the advantage of using LQG is that, in contrast to classical techniques, it naturally enables the development of higher performance centralized controllers in a design process in which the complexity of the synthesized controllers are increased in order to achieve greater performance. The benefits of this type of design process are clearly demonstrated in the results of Ref. 5. Centralized controllers were not designed in this project due to the unavailability of adequate multi-input, multi-output models of the HST.

The paper is organized as follows. Section II describes the HST control design problem. Section III describes the models provided by MSFC for control design and simulation and discusses the rationale for choosing the "composite" models for control design. Section IV then discusses some of the basic issues in applying modern control design to the HST and describes the control approach actually used. The following section then describes a reduced-order LQG controller designed for the HST and uses on-orbit data to compare its performance with that of the original PID-type controller and a previously designed modified HST controller. Section V presents some conclusions.

II. Hubble Space Telescope Control Problem

The HST (see Fig. 1) is a 2.4-m-diam Ritchie-Critien-type Cassegrainian telescope currently in an Earth orbit. This telescope operates as an international astronomical facility. The HST includes two sets of flexible appendages: two solar arrays and two high-gain antennas.

The sensors used for the pointing control system (PCS) are a set of six rate gyro assemblies (RGAs). To provide system redundancy, the RGAs are skewed with respect to the HST vehicle frame, defined by the V_1, V_2, and V_3 axes shown in Fig. 1. Only four RGAs are used at a given time for actual control law implementation. Each RGA has a bandwidth of 18 Hz.

The actuators used for the PCS consist of four reaction wheel assemblies (RWAs). Similar to the RGAs, the spin axes of these RWAs are skewed relative to the HST vehicle frame. Each RWA has a torque bandwidth exceeding 50 Hz and a software-limited torque capability of 0.82 N-m.

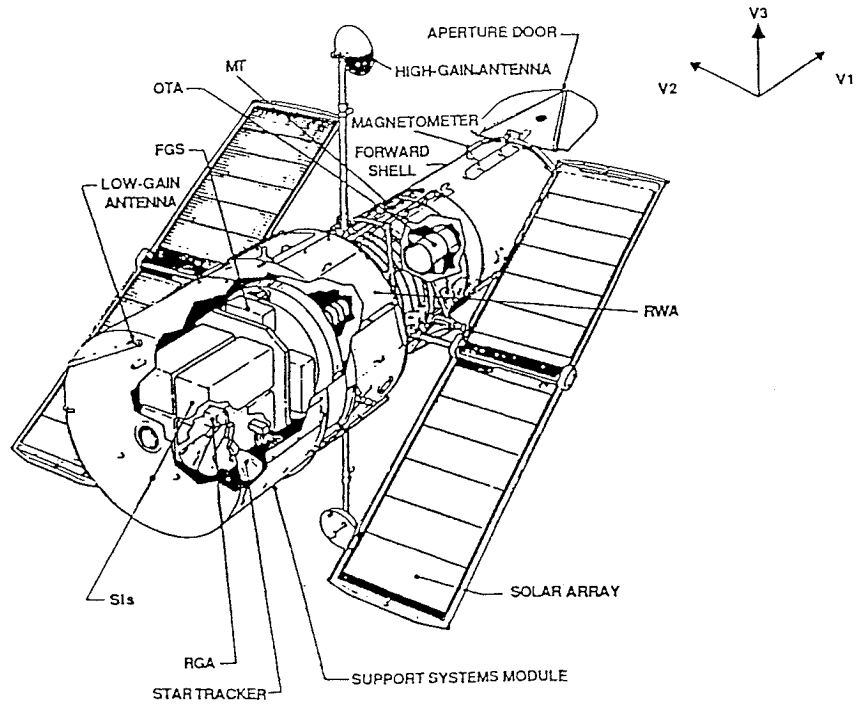

Fig. 1 Hubble space telescope.

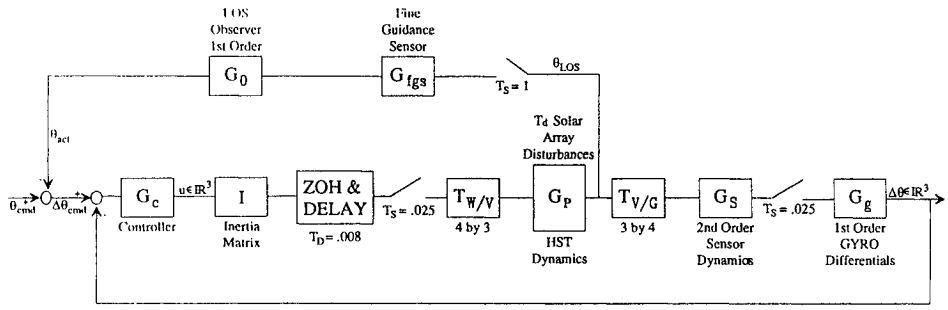

Fig. 2 Block diagram of control configuration for HST.

A block diagram of the closed-loop control scheme is shown in Fig. 2. The 4×3 transformation matrix $T_{W/V}$ and the 3×4 transformation matrix $T_{V/G}$ essentially decouple the PCS attitude controller into three parallel, single-axis loops. This decoupling would be exact if the HST was a rigid body, but due to the presence of flexible modes, some cross-coupling does exist. The controller is labeled G_c in Fig. 2. The original controller was essentially a PID controller that was not designed to attenuate the effects of the solar array disturbances T_d. This controller has a tracking bandwidth of 0.1 Hz. It is desired to design a new controller G_c that attenuates the effects of the solar array disturbances while maintaining the 0.1-Hz tracking bandwidth of the original PID controller.

By using the original PID controller as the baseline, the disturbance attenuation requirements of the new controller can be formulated as follows.[1] Improve the disturbance rejection at 0.1 Hz by at least a factor of 30 (29.5 dB) and improve the disturbance rejection at 0.6 Hz by at least a factor of 10 (20 dB).

III. Hubble Space Telescope Models

The HST models used for control design and analysis were supplied by MSFC. Essentially, two types of models were provided. The first type consisted of multi-input, multi-output (MIMO) models generated by TREETOPS, a multibody dynamic analysis and simulation program. Three models were provided from TREETOPS, corresponding to solar array orientations of 0 deg, 45 deg, and 105 deg. These models differed significantly, as illustrated in Fig. 3, which shows the magnitude frequency response of the single-input, single-output (SISO) transfer function from the V_3 reaction wheel to the V_3 rate gyro.

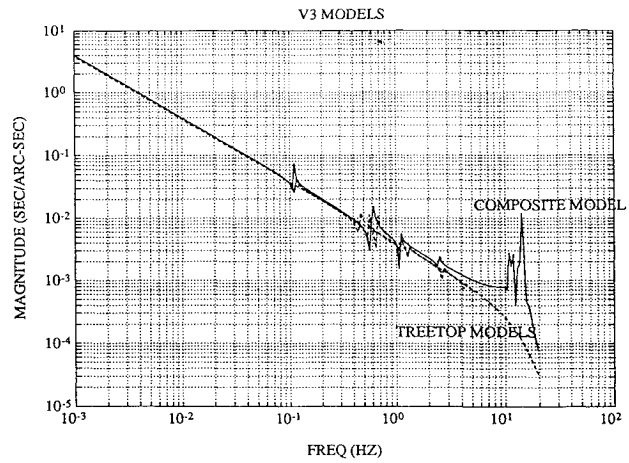

Fig. 3 Magnitude frequency response of 0, 45, and 105 deg, and composite models for V_3 axis.

In addition to the TREETOPS models, MSFC provided SISO modal models of the three dominant transfer functions. These models were designed to represent an average of the transfer functions corresponding to the various solar array orientations and are thus called composite models. The frequency response of the composite model about the V_3 axis is shown in Fig. 3. Notice that the composite model contains modes above 10 Hz, both of which are "scissor" modes, whereas the TREETOPS models do not include these modes. This highlights a major difference between the two sets of models. In

the control designs discussed here, the SISO composite models were chosen for control design. This of course restricted the controllers to be SISO.

The choice of composite models was motivated by several considerations. First, the transformed plant is approximately decoupled. Hence, the performance achievable using SISO designs should be close to the performance achievable using MIMO design. It is also possible that the mode shape (or eigenvector) changes of the plant as the solar orientations change are so great that it is not possible to use MIMO design to significantly improve the performance achievable with SISO control. What is more certain is that SISO designs are fault tolerant and are thus safer to implement on orbit. In addition, the composite models contain the high-frequency scissor modes. These modes really exist and should be present in the control design model(s) to avoid destabilizing these modes when the controller is actually implemented.

IV. Control Approaches

Any controllers implemented must satisfy essentially three criteria:

1) They must provide good tracking from direct current (dc) to 0.1 Hz and contain a double integrator (as did the original PID controllers).

2) They must substantially improve the disturbance rejection properties of the original PID controllers around 0.1 and 0.6 Hz. Specifically, as previously mentioned, they must improve the disturbance rejection at 0.1 Hz by at least a factor of 30 (29.5 dB) and improve the disturbance rejection at 0.6 Hz by at least a factor of 10 (20 dB).

3) They must contain 42 states or less to meet the processor throughput requirements.

Tracking/Integral Control

At this point we assume that $G(s)$ is a w-plane representation of the plant transfer function from u_i to $\Delta\theta_i$, where $i = 1, 2, 3$. The transfer function $G(s)$ represents a type-1 system since it contains a single integrator. To reject very low frequency disturbances due to aerodynamic drag and gravity gradients and to retain the interface to the existing HST attitude observer loop, the controller is required to have two integrators. In addition, this controller is required to have a bandwidth that yields good tracking from dc to 0.1 Hz. LQG control design can be used to attempt the design of such a controller by posing the disturbance rejection problem shown in Fig. 4. In the stochastic interpretation of LQG design $W_T(s)$ is a white-noise disturbance with unit intensity, and hence $r(s)$, the signal to be tracked, is modeled as colored noise. The variable $y(s)$ is the output of the plant. The objective is to regulate the error $r(s) - y(s)$. This type of an approach was used successfully in a tracking problem associated with the ACES (Active Control for Experimental Structures) testbed at MSFC.[4]

The critical issue is how to choose the disturbance filter $T(s)$ in Fig. 4 to force the controller $G_c(s)$ to have the desired number

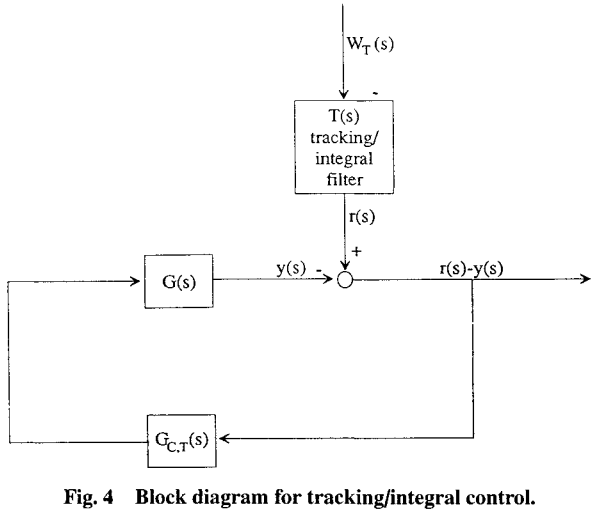

Fig. 4 Block diagram for tracking/integral control.

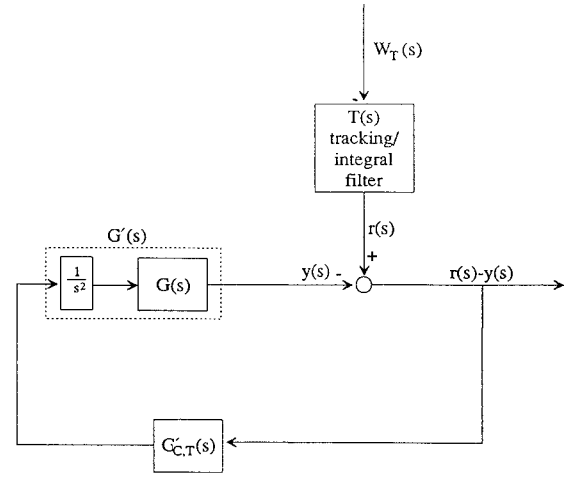

Fig. 5 Controller design for tracking/integral control using precompensation methodology.

of integrators (in this case two) and to also achieve the desired tracking bandwidth. The initial impulse might be to choose $T(s) = (1/s^2)T'(s)$, where $T'(s)$ does *not* contain any poles at the origin. The idea is that the number of integrators in $G_{c,T}(s)$ will be equal to the number of integrators in $T(s)$. However, one problem with this is that, in an LQG context, this choice of $T(s)$ leads to an ill-posed problem since the design model would have uncontrollable, neutrally stable poles. A compromise formulation is to choose $T(s) = [1/(s + \varepsilon_1)^2]T'(s)$, where ε_1 is chosen very small. One might expect this to lead to a compensator of the form $G_{c,T}(s) = [1/(s + \varepsilon_2)^2]G_{c,T'}(s)$. Experimentally, it has been seen that this is true *if* there are no rigid-body modes in the plant $G(s)$. The general rule of thumb is as follows: After an LQG design, the number of integrators and pseudointegrators [i.e., $1/(s + \varepsilon)$] in the product $G(s)G_c(s)$ is equal to the number of pseudointegrators in the disturbance filter $T(s)$.

Since the plant $G(s)$ corresponding to one of the composite models has one integrator and two integrators were desired in the controller, $T(s)$ was actually chosen to be of the form

$$T(s) = 1/(s + \varepsilon)^3(s + \alpha)$$

where the value of α reflects the desired tracking bandwidth. If $G_{c,T}(s)$ contains integrators (or pseudointegrators), then the corresponding input costs can be very large. This tends to lead to numerical ill-conditioning in the LQG Riccati equation solvers. To avoid this, as shown in Fig. 5, a precompensation methodology can be used to imbed the desired number of controller integrators in a modified design plant $G'(s)$ so that the corresponding LQG compensator $G_{c,T'}(s)$ actually contains no integrators (or pseudointegrators). Then, as shown in Fig. 6, the integrators are appended to $G_{c,T'}(s)$ to obtain the controller actually implemented. This type of precompensation strategy was previously used to design controllers for the Mini-MAST structure at NASA Langley Research Center[5] and a popular benchmark problem.[6]

Once $G_{c,T'}(s)$ is designed using LQG, it is often easy to reduce in order using balanced controller reduction[7] or pole-zero deletions based on approximate pole-zero cancellations. Subsequently, its very low frequency zeros can be deleted and very low frequency poles replaced with poles at the origin so that $G_c(s)$ actually contains the desired number of true integrators (in this case two).

Simultaneous Design for Tracking/Integral Control and Disturbance Rejection

Simultaneous tracking/integral control and higher frequency disturbance rejection can be accomplished as shown in Fig. 7 by adding an additional disturbance path to the feedback configuration of Fig. 5. All variables in Fig. 7 that also appear in Fig. 5 have the same interpretation as discussed above for Fig. 5. In addition, in LQG design $W_D(s)$ is a white-noise disturbance with unit intensity, and

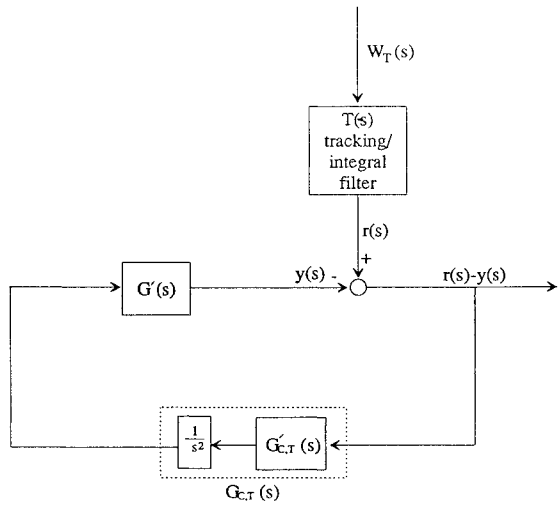

Fig. 6 Controller implementation for tracking/integral control using a precompensation methodology.

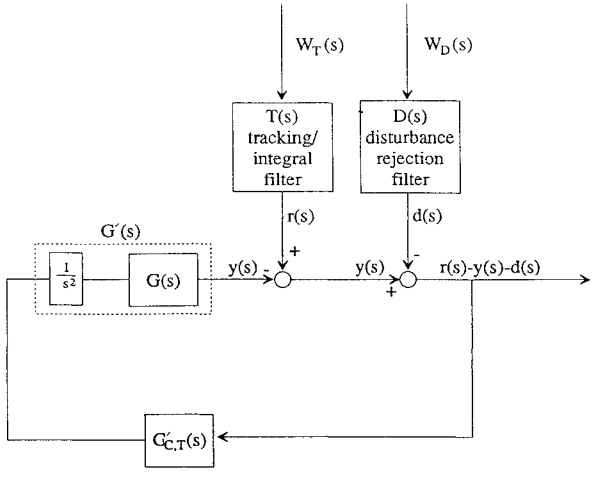

Fig. 7 Block diagram for simultaneous tracking/integral control and disturbance rejection.

hence $d(s)$, the filtered disturbance, is modeled as colored noise. The approach of Fig. 7 appears to have promise but was complicated and somewhat ill-conditioned due to the presence of the low-frequency dynamics appearing in the tracking/integral filter as described above.

The complications of this approach were largely due to the difficulty in choosing the linear quadratic cost function to judiciously emphasize the relative importance of the tracking and disturbance rejection requirements. Because of this difficulty and also (to a lesser degree) because of numerical ill-conditioning due to the low-frequency poles in the tracking/integral filter, high-performance control laws were difficult to achieve. These problems led to the method of separately designing for higher frequency disturbance rejection as described below.

Disturbance Rejection Design Subsequent to Tracking/Integral Design

In this approach, which we found to be simpler to implement, the disturbance rejection compensator acts on the closed-loop plant, which includes the tracking controller $G_{c,T}(s)$ (see Fig. 8). This closed-loop plant does not have the very low frequency dynamics that cause numerical conditioning problems. The tracking controller $G_{c,T}(s)$ and the disturbance rejection controller $G_{c,D}(s)$ can be implemented as a single compensator in the forward path $G_c(s)$, where

$$G_c(s) = G_{c,T}(s) + G_{c,D}(s)$$

To achieve the disturbance rejection requirements using this approach, we found it beneficial to increase the gain on the tracking

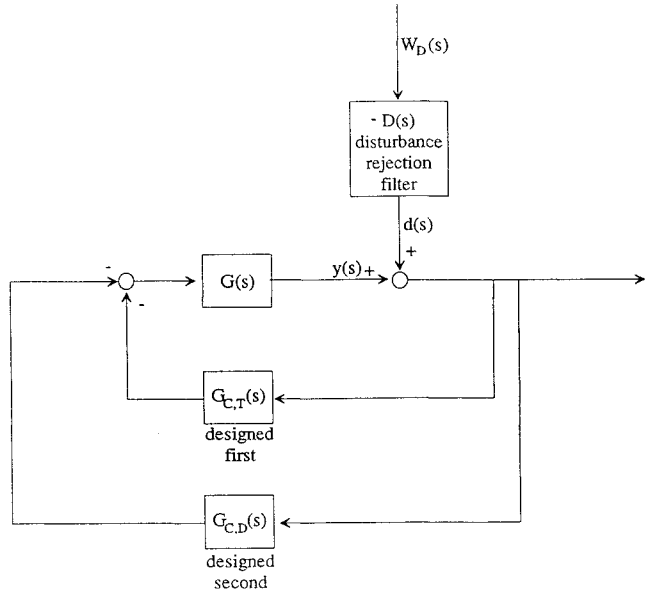

Fig. 8 Block diagram for designing for disturbance rejection.

controller $G_{c,T}(s)$ before designing the disturbance rejection controller $G_{c,D}(s)$. Hence $G_{c,T}(s)$ in Fig. 8 was replaced by $\beta G_{c,T}(s)$ for some $\beta > 1$ and $G_c(s)$ is given by

$$G_c(s) = \beta G_{c,T}(s) + G_{c,D}(s)$$

V. Reduced-Order LQG Controller for HST

Now, we describe a reduced-order LQG controller that meets the performance objectives for vibration suppression of the HST. Since the performance objectives are not influenced by the LOS about the V_1 axis, we will use the original (seventh order) PID-type controller to control this axis while designing modified controllers for the V_2 and V_3 axes. It was found in the design process that the controllers designed for the V_2 and V_3 axes are very similar, so that a high-performance controller designed for the V_2 axis also yields high performance for the V_3 axis. Hence, we chose to design for the V_2 axis and use an identical controller for the V_3 axis. A similar design philosophy was used in Ref. 1.

The controllers were designed using the two-step approach described above. In particular, we designed in succession a tracking/integral controller and then a disturbance rejection controller. LQG design was used to design a tracking controller, $G_{c,T}(s)$, which was easily reduced to a second-order controller using pole-zero deletions. Balanced controller reduction[7] was attempted, but due to the presence of the low-frequency dynamics in the tracking/integral filter $T(s)$, the controllability and observability grammians used for balanced controller reduction were ill-conditioned and the balancing algorithm failed. The dynamics of $G_{c,T}(s)$ are given by

$$G_{c,T}(s) = 279.14(s + 0.050824)(s + 2.4586)/s^2$$

The disturbance rejection controller $G_{c,D}(s)$ was designed using a 33rd-order design model that, as shown in Fig. 8, included the dynamics of the tracking/integral controller $G_{c,T}(s)$. The disturbance rejection filter $D(s)$ was chosen to have the magnitude frequency response shown in Fig. 9 and emphasized the importance of rejecting disturbances at 0.1 and 0.4 Hz. The dynamics of $G_{c,D}(s)$ were reduced to 13th order via pole-zero deletions. (Again balanced controller reduction was numerically sensitive due to the conditioning of the problem.) The final controller, $H(s) = G_{c,T}(s) + G_{c,D}(s)$ is 15th order and has the frequency response shown in Fig. 10. As shown in Figs. 11 and 12, the controller met the performance objectives of improving the disturbance rejection at 0.1 Hz by at least 30 dB and improving the disturbance rejection at 0.6 Hz by at least 20 dB. It is evident by comparing the reduced-order LQG controller with the original PID-type controller that the LQG controller improves the tracking properties of the original PID-type controllers

from dc to 0.1 Hz. Since the total order of the compensator that controls the V_1, V_2 and V_3 axes is 37, the dimension of the compensator meets the requirement of having fewer than 42 states.

The performances of the PID-type controller, the solar array gain augmentation (SAGA-II) controller of Ref. 1, and the LQG controller were also evaluated using on-orbit data as described in Ref. 1. Figures 13 and 14 show the power spectral densities (PSDs) of the outputs for each of these controllers, whereas Table 1 lists the root-

Table 1 Root-mean-square and peak LOS values

Controller	$V_{2,\text{rms}}$, arc-s	$V_{2,\text{peak}}$, arc-s	$V_{3,\text{rms}}$, arc-s	$V_{3,\text{peak}}$, arc-s
PID	34.77	108.2	34.97	122.5
SAGA-II	4.538	37.77	6.053	34.09
LQG	5.083	40.79	5.407	26.19

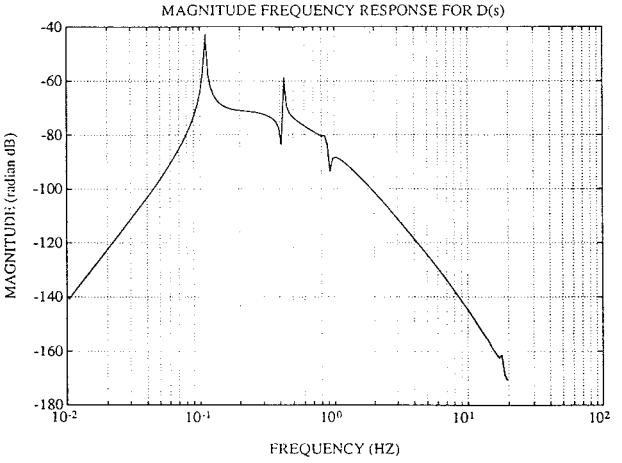

Fig. 9 Magnitude frequency response of disturbance rejection filter $D(s)$.

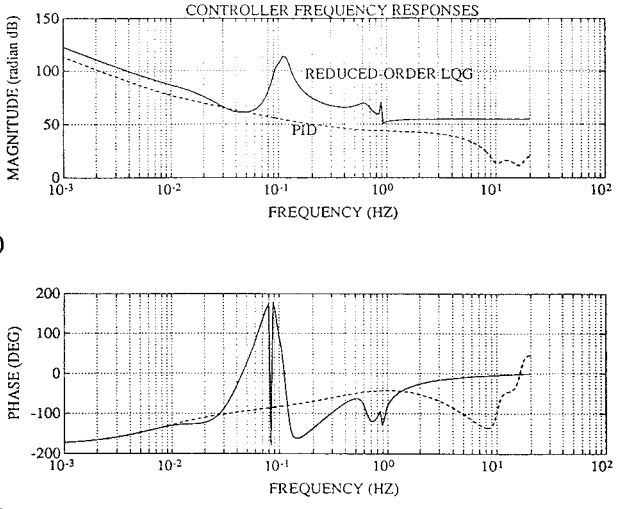

Fig. 10 Frequency responses of PID-type and reduced-order LQG controllers.

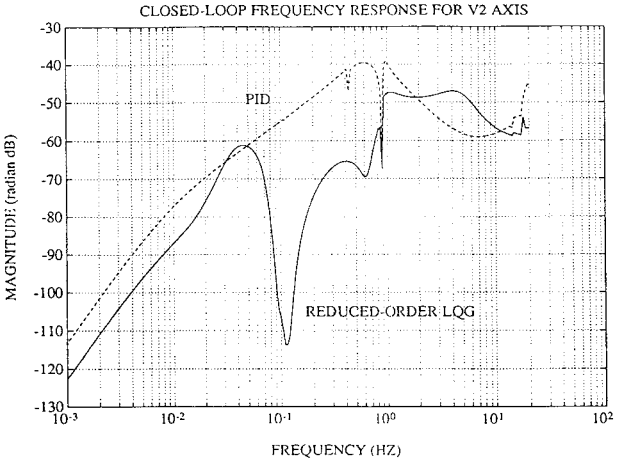

Fig. 11 Closed-loop frequency response for V_2 axis.

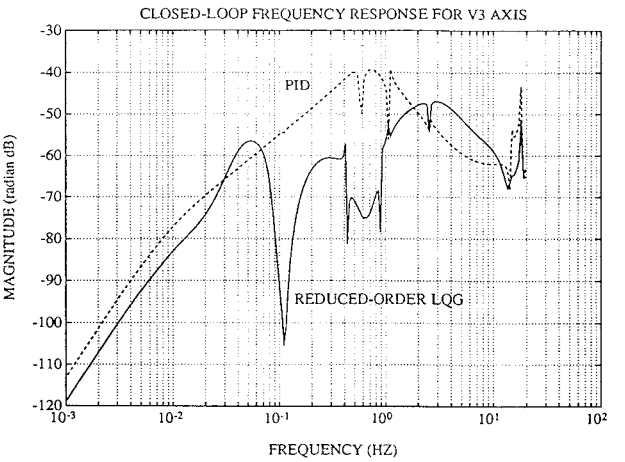

Fig. 12 Closed-loop frequency response for V_3 axis.

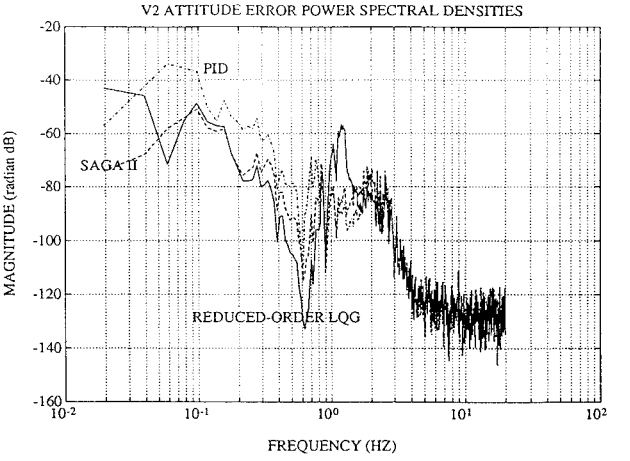

Fig. 13 LOS PSD for V_2 axis.

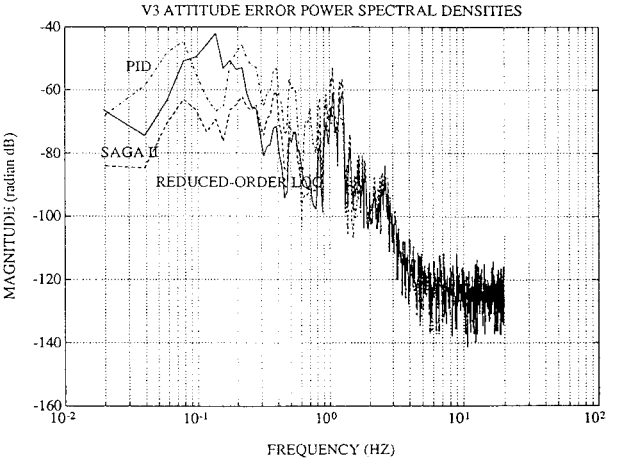

Fig. 14 LOS PSD for the V_3 axis.

mean-square (rms) and peak values of the LOSs. Table 1 and Figs. 13 and 14 show that the performance of the LQG-based compensator is comparable to the performance of the SAGA-II compensator.

It should be acknowledged that, although the plant used in the simulations resulting in Table 1 and Figs. 13 and 14 differed from the actual design plant, hence indicating some robustness of the LQG compensator, the robustness of the compensator to changes in the plant dynamics was not thoroughly analyzed. If a more robust controller is needed, this can be accomplished by using a generalized LQG design technique such as maximum-entropy design,[5,6,8,9] which will enable the modification of the original LQG controller to achieve the desired robustness characteristics. The robustness properties of each controller can be rigorously analyzed using Popov robustness analysis.[10,11]

VI. Conclusions

This paper has considered the design of vibration attenuation controllers for the HST using LQG-based design. Two alternative design approaches were considered, a one-step design procedure and a two-step design procedure in which the disturbance rejection controller is designed subsequent to the integral controller. The latter approach was ultimately used to design a reduced-order LQG controller due to the presence of greater ill-conditioning in the two-step procedure. A resultant controller is described, and its performance is shown to meet the stated performance requirements.

We attempted to use balanced controller reduction to reduce the order of the LQG controller, but this approach failed due to numerical ill-conditioning in the controllability and observability grammians. Hence, pole-zero deletions were used to perform the order reduction. The observed ill-conditioning was apparently due to the integrators appearing in the tracking/integral controller $G_{c,I}(s)$. The numerical problems encountered motivates the search for more numerically robust modern control algorithms.

Acknowledgment

This work was sponsored by NASA Marshall Space Flight Center under Contract NAS8-38575.

References

[1]Sharkey, J. P., Nurre, G. S., Beals, G. A., and Nelson, J. D., "A Chronology of the On-Orbit Pointing Control System Changes on the Hubble Space Telescope and Associated Pointing Improvements," *Proceedings of the 1992 AIAA Guidance, Navigation, and Control Conference* (Hilton Head Island, SC), AIAA, Washington, DC, 1992.

[2]Athans, M., "The Role and Use of the Stochastic Linear-Quadratic-Gaussian Problem in Control System Design," *IEEE Transactions on Automatic Control*, Vol. 23, 1971, pp. 529–552.

[3]Kwakernaak, H., and Sivan, R., *Linear Optimal Control Systems*, Wiley, New York, 1972.

[4]Collins, E. G., Jr., Phillips, D. J., and Hyland, D. C., "Robust Decentralized Control Laws for the ACES Structure," *Control Systems Magazine*, Vol. 11, 1991, pp. 62–70.

[5]Collins, E. G., Jr., King, J. A., Phillips, D. J., and Hyland, D. C., "High Performance, Accelerometer-Based Control of the Mini-MAST Structure," *Journal of Guidance, Control, and Dynamics*, Vol. 15, 1992, pp. 885–892.

[6]Collins, E. G., Jr., King, J. A., and Bernstein, D. S., "Application of Maximum Entropy/Optimal Projection Design Synthesis to a Benchmark Problem," *Journal of Guidance, Control, and Dynamics*, Vol. 15, 1992, pp. 1094–1102.

[7]Yousuff, A., and Skelton, R. E., "A Note on Balanced Controller Reduction," *IEEE Transactions on Automatic Control*, Vol. AC-29, 1984, pp. 254–256.

[8]Bernstein, D. S., and Hyland, D. C., "Maximum Entropy Stochastic Approach to Controller Design for Uncertain Structural Systems," *Proceedings of the American Control Conference*, Inst. of Electrical and Electronics Engineers, Piscataway, NJ, 1982, pp. 680–688.

[9]Collins, E. G., Jr., Phillips, D. J., and Hyland, D. C., "Robust Decentralized Control Laws for the ACES Structure," *Control Systems Magazine*, April 1991, pp. 62–70.

[10]Haddad, W. M., and Bernstein, D. S., "Parameter-Dependent Lyapunov Functions, Constant Real Parameter Uncertainty, and the Popov Criterion in Robust Analysis and Synthesis: Part 1, Part 2," *Proceedings of the IEEE Conference on Decision and Control*, Inst. of Electrical and Electronics Engineers, Piscataway, NJ, 1991, pp. 2274–2279, 2618–2623.

[11]Collins, E. G., Jr., Haddad, W. M., and Davis, L. D., "Riccati Equation Approaches for Small Gain, Positivity, and Popov Robustness Analysis," *Journal of Guidance, Control, and Dynamics*, Vol. 17, No. 2, 1994, pp. 322–329.